

Thermal Stability of Magnetized, Optically Thin, Radiative Cooling-dominated Accretion Disks

Xiao-Fei Yu, Wei-Min Gu, Tong Liu, Ren-Yi Ma, and Ju-Fu Lu

*Department of Astronomy and Institute of Theoretical Physics and Astrophysics,
Xiamen University, Xiamen, Fujian 361005, China*

guwm@xmu.edu.cn

ABSTRACT

We investigate the thermal stability of optically thin, two-temperature, radiative cooling-dominated accretion disks. Our linear analysis shows that the disk is thermally unstable without magnetic fields, which agrees with previous stability analysis on the Shapiro-Lightman-Eardley disk. By taking into account the effects of magnetic fields, however, we find that the disk can be or partly be thermally stable. Our results may be helpful to understand the outflows in optically thin flows. Moreover, such radiative cooling-dominated disks may provide a new explanation of the different behaviors between black hole and neutron star X-ray binaries on the radio/X-ray correlation.

Subject headings: accretion, accretion disks - black hole physics - instabilities - magnetic fields - stars: winds, outflows

1. Introduction

Accretion of rotating matter onto a compact object can provide a large amount of released energy and is therefore believed to be the source of cataclysmic variables, X-ray binaries, and active galactic nuclei (AGN). The most famous accretion model is the geometrically thin and optically thick disk (SSD) introduced by Shakura & Sunyaev (1973). Thermal instability was found in the inner region of SSD (Piran 1978) and such an issue has been widely studied by linear analysis and numerical simulations (Hirose et al. 2009; Lin et al. 2011, 2012; Xue et al. 2011; Jiang et al. 2013; Zhu & Narayan 2013). For stellar-mass black holes, the temperature in such a standard disk is in the range $10^4 - 10^7$ K, which is quite low relative to the virial temperature. In order to explain the hard X-ray spectra of black hole X-ray binaries such as Cyg X-1, Shapiro, Lightman & Eardley (1976) introduced

an optically thin, two-temperature disk model (hereafter SLE disk) with $T_e \sim 10^9 \text{K}$. Unfortunately, shortly after the SLE disk was introduced, it was found that the disk is thermally unstable (Pringle 1976; Piran 1978). Both of the above two models are radiative cooling dominated, i.e., the advective energy is negligible.

On the other hand, the energy released through dissipation may be trapped within the accreted gas and then transported in the radial direction towards the central object or stored in the flow as entropy. Such accretion flows can be divided into two types, namely the slim disk and the advection-dominated accretion flow (ADAF). The slim disk was introduced by Abramowicz et al. (1988), which is optically thick with extremely high mass accretion rates. Recently, simulations on the slim disk have revealed that strong outflows may occur (e.g., Ohsuga et al. 2005; Ohsuga & Mineshige 2011; Yang et al. 2014). Moreover, the radiative efficiency is not low and the luminosity can be far beyond the Eddington one (Jiang et al. 2014). The ADAF model was proposed by Narayan & Yi (1994), which is optically thin with low accretion rates. The temperature of ADAF is close to the virial one, which is significantly higher than that in the SLE disk due to energy advection. Simulations on the ADAF have been studied by many previous works (Narayan et al. 2012; Yuan et al. 2012a,b; for a review see Yuan & Narayan 2014). Different from the stability of the SLE disk, both the slim disk and the ADAF are thermally stable due to the dominant energy advection (Abramowicz et al. 1995). A recent work (Gu 2014), however, showed that the advective cooling cannot balance the viscous heating, and therefore outflows ought to be inevitable in such an accretion system.

The stability properties of accretion disks are of importance because a global violently unstable disk may not exist in nature and some instabilities restricted in a certain region of the disk may contribute to the observed light variations in many systems. Since the classic SLE disk was proved to be thermally unstable, such a type of accretion disk is unlikely to be realized in nature. It is generally believed that magnetic fields have fundamental influence on the physics of accretion disks. For example, magnetorotational instability (MRI) is known as a generator of turbulence, through which the angular momentum can be transferred outwards (Balbus & Hawley 1991). Oda et al. (2009, 2010) presented a new thermal equilibrium solution for optically thin disks by incorporating toroidal magnetic fields. They argued that an optically thin, magnetic pressure-dominated accretion disk (low- β disk) will be thermally stable. Zheng et al. (2011) revisited the thermal stability of standard thin disks by including the role of toroidal magnetic fields. Their calculation is based on the assumption of the perturbation relation $\delta B_\phi / B_\phi = -\gamma \delta H / H$, where γ is positive, i.e., the magnetic field will become weaker with increasing height (or temperature). This assumption is supported by the MHD simulation of Machida et al. (2006) for a hot accretion flow, where they found that the magnetic field becomes stronger when the disk shrinks vertically. In addition, the

large-scale magnetic fields in accretion disks have been widely investigated and the strength may be underestimated particularly for the region near the black hole (Cao 2011).

In this paper, we will analyze the thermal stability of optically thin disks by including the role of magnetic fields. The effects of such magnetic fields can be taken into account by modifying the pressure as the sum of the gas pressure and the magnetic pressure: $p = p_{\text{gas}} + p_{\text{mag}}$, $p_{\text{mag}} \sim B^2 \sim \rho^{4/3}$ (Narayan & Yi 1995; Yamasaki 1997). We have to consider two-temperature plasma in such disks because the electron temperature is expected to be significantly lower than the ion temperature in such a low density, high temperature region. In addition, the radiative cooling process is assumed to be the thermal bremsstrahlung. The paper is organized as follows. The basic equations are presented in Section 2. In Section 3, the thermal stability is investigated by linear analysis. In Section 4, the thermal equilibrium curve is obtained by numerical calculation. Conclusions and discussion are made in Section 5.

2. Equations

We consider a steady state, optically thin, two-temperature black hole accretion flows incorporating magnetic fields. We assume the angular velocity is Keplerian, i.e., $\Omega = \Omega_K$. The disk structure is described by the following equations. The continuity equation takes the form:

$$\dot{M} = -4\pi R H \rho v_R, \quad (1)$$

where R is the cylindrical radius, ρ the mass density of the accreted gas, H the half-thickness of the flow, v_R the radial velocity, which is defined to be negative when the flow is inward, and \dot{M} the mass accretion rate. The equation of vertical hydrostatic equilibrium can be written as

$$H = \frac{1}{\Omega_K} \left(\frac{p}{\rho} \right)^{\frac{1}{2}}, \quad (2)$$

where p is the pressure. The Keplerian angular velocity Ω_K takes the form $\Omega_K^2 = GM/(R - R_g)^2 R$, where the gravitational potential of the central black hole is assumed to be $\Phi(R) = -GM/(R - R_g)$, which was introduced by Paczyński & Wiita (1980), with M being the black hole mass and R_g the gravitational radius, $R_g \equiv 2GM/c^2$. From the angular momentum equation we can obtain the expression of the radial velocity (e.g., Gu et al. 2006; Liu et al. 2007),

$$v_R = \frac{\nu R^2}{\Omega R^2 - j} \frac{d\Omega}{dR}, \quad (3)$$

where ν is the kinetic viscosity coefficient, and j represents the specific angular momentum per unit mass accreted by the black hole.

Since the radiation pressure is negligible in optically thin disks, the total pressure p is expressed as

$$p = p_{\text{gas}} + p_{\text{mag}} , \quad (4)$$

where $p_{\text{gas}} = (1 - \beta_{\text{mag}})p$ is the gas pressure, $p_{\text{mag}} = \beta_{\text{mag}}p$ the magnetic pressure. The gas is assumed to consist of protons and electrons and therefore the gas pressure p_{gas} is written as

$$p_{\text{gas}} = \frac{k_{\text{B}}}{\mu m_{\text{p}}} \rho (T_{\text{i}} + T_{\text{e}}) , \quad (5)$$

where k_{B} is the Boltzmann constant, μ the mean molecular weight ($\mu = 1$), m_{p} the proton mass, and T_{i} , T_{e} the ion and electron temperature, respectively.

To construct the energy equations, we introduce the following assumptions: i) the dissipation energy goes into the ions; ii) the energy is transferred from the ions to the electrons through the Coulomb coupling; iii) the electrons are cooled by the bremsstrahlung process. Based on these assumptions, the energy equations of the ions and electrons can be respectively written as

$$q_{\text{vis}}^+ = \Lambda_{\text{ie}} , \quad (6)$$

$$\Lambda_{\text{ie}} = q_{\text{e}}^- , \quad (7)$$

where q_{vis}^+ is the viscous heating rate per unit volume, Λ_{ie} the energy transfer rate from the ions to the electrons per unit volume, q_{e}^- the radiative cooling rate of electrons per unit volume. The viscous heating rate can be written as

$$q_{\text{vis}}^+ = \rho \nu \left(R \frac{d\Omega}{dR} \right)^2 . \quad (8)$$

We adopt the standard α prescription in this paper, i.e., $\nu = \alpha c_{\text{s}} H$, where $c_{\text{s}} \equiv (p/\rho)^{1/2}$ and α is a constant parameter. Λ_{ie} is given by Stepney & Guilbert (1983):

$$\Lambda_{\text{ie}} = \frac{3}{2} \frac{m_{\text{e}}}{m_{\text{i}}} n^2 \sigma_{\text{T}} c (\ln \Lambda) \frac{kT_{\text{i}} - kT_{\text{e}}}{K_2(1/\Theta_{\text{i}}) K_2(1/\Theta_{\text{e}})} \left[\frac{2(\Theta_{\text{i}} + \Theta_{\text{e}})^2 + 1}{\Theta_{\text{i}} + \Theta_{\text{e}}} K_1 \left(\frac{\Theta_{\text{i}} + \Theta_{\text{e}}}{\Theta_{\text{i}} \Theta_{\text{e}}} \right) + 2K_0 \left(\frac{\Theta_{\text{i}} + \Theta_{\text{e}}}{\Theta_{\text{i}} \Theta_{\text{e}}} \right) \right] , \quad (9)$$

where σ_{T} is the Thomson scattering cross section and $\ln \Lambda$ is the Coulomb logarithm (roughly $\ln \Lambda \sim 20$). K_n are modified Bessel function of the second kind of the order n , respectively.

The quantities Θ_i and Θ_e are defined as $\Theta_i \equiv k_B T_i / m_p c^2$ and $\Theta_e \equiv k_B T_e / m_e c^2$, where m_p and m_e are the mass of the proton and electron, respectively. For simplicity, we use the following formula which uses no special functions (Kato et al. 2008):

$$\Lambda_{ie} = \frac{3}{2} \nu_E \frac{\rho k_B (T_i - T_e)}{m_p}, \quad (10)$$

with the electron-ion coupling being $\nu_E = 2.4 \times 10^{21} (\ln \Lambda) \rho T_e^{-3/2}$.

Following Narayan & Yi (1995), the bremsstrahlung cooling rate per unit volume is

$$q_e^- = q_{br}^- = q_{br,ei}^- + q_{br,ee}^- = n^2 \sigma_T c \alpha_f m_e c^2 [F_{ei}(\Theta_e) + F_{ee}(\Theta_e)], \quad (11)$$

where the subscripts “ei” and “ee” denote the electron-ion and electron-electron bremsstrahlung cooling rates, α_f is fine-structure constant, and the function $F_{ei}(\Theta_e)$ and $F_{ee}(\Theta_e)$ have the approximate form:

$$F_{ei}(\Theta_e) = \begin{cases} \frac{9\Theta_e}{2\pi} \left[\ln(2\eta\Theta_e + 0.48) + \frac{3}{2} \right] & (\Theta_e > 1) \\ 4 \left(\frac{2\Theta_e}{\pi^3} \right)^{1/2} [1 + 1.781\Theta_e^{1.34}] & (\Theta_e < 1) \end{cases}, \quad (12)$$

$$F_{ee}(\Theta_e) = \begin{cases} \frac{9\Theta_e}{\pi} [\ln(2\eta\Theta_e) + 1.28] & (\Theta_e > 1) \\ \frac{5}{6\pi^{3/2}} (44 - 3\pi^2) \Theta_e^{3/2} \times \\ (1 + 1.1\Theta_e + \Theta_e^2 - 1.25\Theta_e^{5/2}) & (\Theta_e < 1) \end{cases},$$

where $\eta = \exp(-\gamma_E)$ and $\gamma_E \approx 0.5772$ is Euler’s number.

3. Thermal stability analysis

The thermal instability criterion of accretion disks can be expressed as (e.g., Frank et al. 1992)

$$\left(\frac{\partial \ln Q^-}{\partial \ln T} \right)_\Sigma < \left(\frac{\partial \ln Q^+}{\partial \ln T} \right)_\Sigma, \quad (13)$$

where Q^+ , Q^- and T are respectively the viscous heating rate, radiative cooling rate, and temperature. Σ is the surface density defined as $\Sigma = 2\rho H$. Such a criterion is identical to that in Piran (1978) if we replace T by H .

Since the disk is two-temperature, the thermal stability analysis should be made for ion and electron temperature modulations, respectively. The cooling timescale of the electron is quite short and therefore the thermal stability of the electron is priority. The surface density Σ is assumed to be unchanged during a thermal timescale, so we have

$$\frac{d \ln \rho}{d \ln T_e} = - \frac{d \ln H}{d \ln T_e} . \quad (14)$$

With Equations (7), (10), (11) and (14), and the assumption that T_i keeps unchanged during the perturbation of T_e , we can obtain

$$\left(\frac{\partial \ln q_e^+}{\partial \ln T_e} \right)_\Sigma - \left(\frac{\partial \ln q_e^-}{\partial \ln T_e} \right)_\Sigma < 0 , \quad (15)$$

where q_e^+ is equal to Λ_{ie} . The above relationship means that the disk is always stable against electron temperature perturbations. Such a result is in agreement with Kato et al. (2008).

If electrons are thermally stable, then we have

$$\frac{d(\ln q_e^+)}{d \ln T_i} = \frac{d(\ln q_e^-)}{d \ln T_i} . \quad (16)$$

With Equation (7) we can obtain the ratio of T_i to T_e as a function of T_e , i.e., a function of Θ_e ,

$$\frac{T_i}{T_e} = g(\Theta_e) . \quad (17)$$

Equation (2) gives

$$\frac{d \ln p}{d \ln T_i} = - \frac{d \ln \rho}{d \ln T_i} . \quad (18)$$

By using Equations (4), (5) and (18), together with the relationship $p_{\text{mag}} \propto \rho^{4/3}$ mentioned in Section 1, we can derive

$$\frac{d \ln \rho}{d \ln T_i} = - \frac{3(1 - \beta_{\text{mag}})}{6 + \beta_{\text{mag}}} \frac{d \ln(T_i + T_e)}{d \ln T_i} , \quad (19)$$

then with Equations (16), (17) and (19) we can obtain

$$\frac{dT_e}{dT_i} = h(\beta_{\text{mag}}, \Theta_e) . \quad (20)$$

Equations (6), (8) and (10) can provide

$$\frac{d \ln(q_i^+ - q_i^-)}{d \ln T_i} = -3 \frac{d \ln \rho}{d \ln T_i} - \frac{d \ln(T_i - T_e)}{d \ln T_i} + \frac{3}{2} \frac{d \ln T_e}{d \ln T_i} . \quad (21)$$

Substituting Equations (17), (19) and (20) into Equation (21), we finally get

$$\left[\frac{\partial \ln(q_i^+ - q_i^-)}{\partial \ln T_i} \right]_{\Sigma} = f(\beta_{\text{mag}}, \Theta_e), \quad (22)$$

then the thermal instability criterion can be expressed as $f(\beta_{\text{mag}}, \Theta_e) > 0$. Detailed expressions of $g(\Theta_e)$, $h(\beta_{\text{mag}}, \Theta_e)$, and $f(\beta_{\text{mag}}, \Theta_e)$ are presented in the Appendix.

Figure 1 shows the variation of the function $f(\Theta_e)$ for a certain given value of β_{mag} . It is seen that for $\beta_{\text{mag}} = 0$, i.e., no magnetic field, $f(\Theta_e)$ is positive for any Θ_e , which means that the disk will be thermally unstable. This result agrees with previous stability analysis on the SLE disk. Actually, for $\beta_{\text{mag}} = 0$, the equations will reduce to that for SLE disks. The interesting result is that for $\beta_{\text{mag}} = 0.7$, $f(\Theta_e)$ is negative for any Θ_e , which implies that the disk will be thermally stable. For the typical equipartition case $\beta_{\text{mag}} = 0.5$, the figure shows that there exists a thermally stable region corresponding to $0.03 \lesssim \Theta_e \lesssim 1$, whereas for $\Theta_e \lesssim 0.03$ or $\Theta_e \gtrsim 1$ the disk will be thermally unstable. In other words, the disk can be or partly be thermally unstable owing to the effects of magnetic fields.

The physical interpretation of thermally stable disks for moderate strength of magnetic fields may be as follows. For a positive perturbation of the ion temperature T_i , the gas pressure p_{gas} will increase and therefore the disk thickness H will also increase. Consequently, the strength of magnetic fields B and the magnetic pressure p_{mag} will decrease due to the increasing volume. Thus, the total pressure ($p_{\text{gas}} + p_{\text{mag}}$) as well as the viscous stress will not increase as fast as in the disk without magnetic fields. Therefore, the viscous heating rate q_{vis}^+ may increase more slowly compared with the case without magnetic fields. In this spirit, it is reasonable that the disk can become thermally stable when the role of magnetic fields is taken into account.

4. Thermal equilibrium solutions

In this section, we will show the numerical calculation of the local thermal equilibrium solutions with Equations (1)-(7), where $M = 10M_{\odot}$, $j = 1.8cR_g$, $\alpha = 0.1$, and $\beta_{\text{mag}} = 0.5$. Figure 2 shows the radial variations of the ion and electron temperature for $\dot{m} = 0.001$, 0.01, and 0.1, where $\dot{m} \equiv \dot{M}/\dot{M}_{\text{Edd}}$ ($\dot{M}_{\text{Edd}} \equiv 16L_{\text{Edd}}/c^2$). It is seen that the ion temperature is significantly higher than the electron temperature in the inner region of the disk. We would like to point out that the temperature in the real case may be lower than the current solutions since only the bremsstrahlung cooling process is taken into consideration. In the classic ADAF model where the radiative cooling is negligible compared with the viscous

heating, there exists a conservation relationship (e.g., Molteni et al. 2001),

$$\frac{1}{2}v_R^2 + \frac{\gamma}{\gamma - 1}\frac{p}{\rho} + \frac{1}{2}\Omega^2 R^2 - \Omega(\Omega R^2 - j) - \frac{GM}{R - R_g} = \lambda, \quad (23)$$

where λ is a constant and should be quite small compared with the terms on the left hand side such as $GM/(R - R_g)$, particularly for small radii. Based on the above equation, we can derive the theoretical ion temperature of ADAF by

$$\frac{5}{2}\frac{k_B T_i}{\mu m_p} = \frac{GM}{R - R_g} + \frac{1}{2}\Omega^2 R^2 - j\Omega, \quad (24)$$

where $\gamma = 5/3$ and $\lambda = 0$ are adopted, and the term $v_R^2/2$ is ignored. The theoretical ion temperature is also plotted in Figure 2 by the navy blue line for a comparison. It is seen that the ion temperature of ADAF is significantly higher than the cooling-dominated disks even for $\dot{m} = 0.1$, which indicates that the energy advection is negligible and our thermal equilibrium solutions are self-consistent.

Figure 3 shows the stable and unstable regions in the $\dot{m} - R$ diagram for $\beta_{\text{mag}} = 0.5$. The region with $f(\Theta_e) < 0$ corresponds to the thermal stable solutions. For a given \dot{m} , the figure clearly shows the thermally stable range in the disk. It is seen that, for a typical accretion rate $\dot{m} = 0.01$, the disk is thermally stable from the inner boundary to $\sim 10^3 R_g$. Such a stable solution may provide a second possibility for the optically thin accretion flows. For higher accretion rates such as $\dot{m} \gtrsim 0.1$ the figure shows an unstable inner region, which implies that outflows are likely to be inevitable and the rate accreted by the black hole is less than 0.1. On the other hand, for low accretion rates such as $\dot{m} \lesssim 0.001$, the disk only has an inner stable part $\lesssim 100 R_g$. A thermally stable disk for such low accretion rates may require stronger magnetic fields, i.e., $\beta_{\text{mag}} \rightarrow 0.7$. Another possibility for the outer part of the disk to be stable may be related to the self-gravity, as argued by Bertin & Lodato (2001).

5. Conclusions and Discussion

In this work, we have investigated the thermal stability of magnetized, optically thin, two-temperature, radiative cooling-dominated accretion disks by linear analysis. We have derived a general criterion for such an instability (Equation 22). We have found that the disk is thermally unstable without magnetic fields, which agrees with previous stability analysis on the SLE disk. On the contrary, for adequately strong magnetic fields with $\beta_{\text{mag}} \sim 0.7$, the whole disk will be thermally stable. For the typical equipartition case, $\beta_{\text{mag}} = 0.5$, the disk has a wide stable region particularly for \dot{m} around 0.01. Our results may be helpful

to understand the mechanism of outflows in optically thin accretion flows, which may be triggered by the thermal instability.

The well-known ADAF model is a classic model, and may be known as the unique stable model for optically thin accretion flows. Since the black hole has a horizon rather than a solid surface, it is easy to understand that the flow will be transonic and the internal energy will eventually be absorbed by the hole. On the contrary, for a neutron star accretion system, since the neutron star has a real surface, it remains uncertain whether the ADAF can still be stable and work well in such a system, particularly for the inner region. The present work provides a second possibility for the optically thin accretion flows, i.e., the magnetized, radiative cooling-dominated disk. In our opinion, since the radiative cooling can balance the viscous heating locally in such a model, the energy advection will be negligible. Thus, such a model may work well for both black hole and neutron star systems.

The observations have shown that the radio and X-ray emission during the hard state are strongly correlated for black hole and neutron star X-ray binaries. Taking the form of non-linear luminosity correlation, there exists the relationship $L_R \propto L_X^b$, where L_R is the radio luminosity and L_X is the X-ray luminosity. For neutron star X-ray binaries, the correlation index is $b \sim 1.4$ (Migliari & Fender 2006). On the contrary, for black hole X-ray binaries, the correlation is quite complex. At first the correlation with $b \sim 0.7$ was obtained based on the data of different sources (e.g., Hannikainen et al. 1998, Corbel et al. 2003, Gallo et al. 2003), Later, however, another relation similar to that of neutron stars, i.e., $b \sim 1.4$, was found for specific sources (e.g., Coriat et al. 2011, Jonker et al. 2012, Ratti et al. 2012). As discussed by Coriat et al. (2011), the steep correlation may indicate that the disk is in the radiatively efficient regime. In our point of view, the above observational results can be easily understood based on our new model. Due to the existence of surface, a neutron star system may prefer to the magnetized, radiative cooling-dominated disk which corresponds to $b \sim 1.4$, whereas a black hole system may have two choices, i.e., either the ADAF or the cooling-dominated one, which corresponds to $b \sim 0.7$ and ~ 1.4 , respectively. In addition, we would point out that, an alternative cooling-dominated model for optically thin flows is the luminous hot accretion flow (LHAF) introduced by Yuan (2001), which is, however, likely to be thermally unstable. Concerning the stability, the magnetized, radiative cooling-dominated disk studied in the present work is more likely to exist than the other radiatively efficient disks.

We thank the referee for helpful comments that improved the paper. This work was supported by the National Basic Research Program of China (973 Program) under grant 2014CB845800, the National Natural Science Foundation of China under grants 11103015, 11222328, 11233006, 11333004, 11473022, and U1331101, the Fundamental Research Funds

for the Central Universities under grant 20720140532, and the Natural Science Foundation of Fujian Province of China under grant 2012J01026.

A. Expressions of thermal stability criterion

In this Appendix, we will derive the detailed expressions of $g(\Theta_e)$, $h(\beta_{\text{mag}}, \Theta_e)$, and $f(\beta_{\text{mag}}, \Theta_e)$, which are mentioned in Section 3.

$$g(\Theta_e) = 1 + \frac{\sigma_T \alpha_f m_e^{3/2} m_p c^4 \Theta_e^{1/2} [F_{\text{ei}}(\Theta_e) + F_{\text{ee}}(\Theta_e)]}{3.6 \times 10^{21} (m_p + m_e)^2 k_B^{3/2} \ln \Lambda} . \quad (\text{A1})$$

We define X_1 , X_2 , Y_1 , Y_2 , and k as follows,

$$\begin{aligned} X_1 &= \Theta_e \left[\ln(2\eta\Theta_e + 0.48) + \frac{3}{2} \right] + 2\Theta_e [\ln(2\eta\Theta_e) + 1.28] , \\ X_2 &= 8(2\Theta_e)^{1/2} (1 + 1.781\Theta_e^{1.34}) + \frac{5}{3} (44 - 3\pi^2) \Theta_e^{3/2} (1 + 1.1\Theta_e + \Theta_e^2 - 1.25\Theta_e^{5/2}) , \\ Y_1 &= [\Theta_e \ln(2\eta\Theta_e + 0.48) + 2\eta\Theta_e^2 / (2\eta\Theta_e + 0.48) + 6\Theta_e + 2\Theta_e \ln(2\eta\Theta_e)] / X_1 , \\ Y_2 &= [5.66\Theta_e^{1.5} + 37.1\Theta_e^{1.84} + 36\Theta_e^{1.5} + 66\Theta_e^{2.5} + 83\Theta_e^{3.5} - 120\Theta_e^4] / X_2 , \\ k &= \frac{3(1 - \beta_{\text{mag}})}{6 + \beta_{\text{mag}}} . \end{aligned}$$

We can derive the following expression:

$$h(\beta_{\text{mag}}, \Theta_e) = \begin{cases} \frac{1/(g(\Theta_e) - 1) - 2k/(g(\Theta_e) + 1)}{1.5 + Y_1 + 1/(g(\Theta_e) - 1) + 2k/(g(\Theta_e) + 1)} & (\Theta_e > 1) \\ \frac{1/(g(\Theta_e) - 1) - 2k/(g(\Theta_e) + 1)}{1.5 + Y_2 + 1/(g(\Theta_e) - 1) + 2k/(g(\Theta_e) + 1)} & (\Theta_e < 1) \end{cases} . \quad (\text{A2})$$

Finally, we obtain

$$f(\beta_{\text{mag}}, \Theta_e) = \frac{3kg(\Theta_e)(1 + h(\beta_{\text{mag}}, \Theta_e))}{(g(\Theta_e) + 1)} + 1.5g(\Theta_e)h(\beta_{\text{mag}}, \Theta_e) - \frac{g(\Theta_e)(1 - h(\beta_{\text{mag}}, \Theta_e))}{(g(\Theta_e) - 1)} , \quad (\text{A3})$$

which is the function introduced in Equation (22).

REFERENCES

- Abramowicz, M. A., Chen, X., Kato, S., Lasota, J.-P., & Regev, O. 1995, *ApJ*, 438, L37
- Abramowicz, M. A., Czerny, B., Lasota, J.-P., & Szuszkiewicz, E. 1988, *ApJ*, 332, 646
- Balbus, S. A., & Hawley, J. F. 1991, *ApJ*, 376, 214
- Bertin, G., & Lodato, G. 2001, *A&A*, 370, 342
- Cao, X. 2011, *ApJ*, 737, 94
- Corbel, S., Nowak, M. A., Fender, R. P., et al. 2003, *A&A*, 400, 1007
- Coriat, M., Corbel, S., Prat, L., et al. 2011, *MNRAS*, 414, 677
- Frank, J., King, A., & Raine, D. 1992, *Accretion Power in Astrophysics* (Cambridge: Cambridge Univ. Press)
- Gallo, E., Fender, R. P., & Pooley, G. G. 2003, *MNRAS*, 344, 60
- Gu, W.-M. 2014, *ApJ*, in press, arXiv:1411.3965
- Gu, W.-M., Liu, T., & Lu, J.-F. 2006, *ApJ*, 643, L87
- Hannikainen, D. C., Hunstead, R. W., Campbell-Wilson, D., Sood, R. K. 1998, *A&A*, 337, 460
- Hirose, S., Krolik, J. H., & Blaes, O. 2009, *ApJ*, 691, 16
- Jiang, Y.-F., Stone, J. M., & Davis, S. W. 2013, *ApJ*, 778, 65
- Jiang, Y.-F., Stone, J. M., & Davis, S. W. 2014, *ApJ*, 796, 106
- Jonker, P. G., Miller-Jones, J. C. A., Homan, J., et al. 2012, *MNRAS*, 423, 3308
- Kato, S., Fukue, J., & Mineshige, S. 2008, *Black-Hole Accretion Disks: Towards a New paradigm* (Kyoto: Kyoto Univ. Press)
- Lin, D.-B., Gu, W.-M., & Lu, J.-F. 2011, *MNRAS*, 415, 2319
- Lin, D.-B., Gu, W.-M., Liu, T., Sun, M.-Y., & Lu, J.-F. 2012, *ApJ*, 761, 29
- Liu, T., Gu, W.-M., Xue, L., & Lu, J.-F. 2007, *ApJ*, 661, 1025
- Loeb, A., Narayan, R., & Raymond, J.C. 2001, *ApJ*, 547, L151
- Machida, M., Nakamura, K.E., & Matsumoto, R. 2006, *PASJ*, 58, 193
- Migliari, S. & Fender, R. P. 2006, *MNRAS*, 366, 79
- Molteni, D., Gerardi, G., & Valenza, M. A. 2001, *ApJ*, 551, L77
- Narayan, R., & Yi, I. 1994, *ApJ*, 444, L13
- Narayan, R., & Yi, I. 1995, *ApJ*, 452, 710

- Narayan, R., Sądowski, A., Penna, R. F., & Kulkarni, A. K. 2012, *MNRAS*, 426, 3241
- Oda, H., Machida, M., K.E., & Matsumoto, R. 2009, *ApJ*, 697, 16
- Oda, H., Machida, M., K.E., & Matsumoto, R. 2010, *ApJ*, 712, 639
- Ohsuga, K., & Mineshige, S. 2011, *ApJ*, 736, 2
- Ohsuga, K., Mori, M., Nakamoto, T., & Mineshige, S. 2005, *ApJ*, 628, 368
- Paczynski, B., & Wiita, P. J. 1980, *A&A*, 88, 23
- Piran, T. 1978, *ApJ*, 221, 652
- Pringle, J.E. 1976, *MNRAS*, 177, 65
- Ratti, E. M., Jonker, P. G., Miller-Jones, J. C. A., et al. 2012, *MNRAS*, 423, 2656
- Shakura, N. I., & Sunyaev, R. A. 1973, *A&A*, 24, 337
- Shapiro, S. L., Lightman, A. P., & Eardley, D. N. 1976, *ApJ*, 204, 187
- Stepney, S., & Guilbert, P.W. 1983, *MNRAS*, 204, 1269
- Xue, L., Sądowski, A., Abramowicz, M. A., & Lu, J.-F. 2011, *ApJS*, 195, 7
- Yamasaki, T. 1997, *PASJ*, 49, 227
- Yang, X.-H., Yuan, F., Ohsuga, K., & Bu, D.-F. 2014, *ApJ*, 780, 79
- Yuan, F. 2001, *MNRAS*, 324, 119
- Yuan, F., Bu, D., & Wu, M. 2012a, *ApJ*, 761, 130
- Yuan, F., & Narayan, R. 2014, *ARA&A*, 52, 529
- Yuan, F., Wu, M., & Bu, D. 2012b, *ApJ*, 761, 129
- Zheng, S.-M., Yuan, F., Gu, W.-M., & Lu, J.-F. 2011, *ApJ*, 732, 52
- Zhu, Y., & Narayan, R. 2013, *MNRAS*, 434, 2262

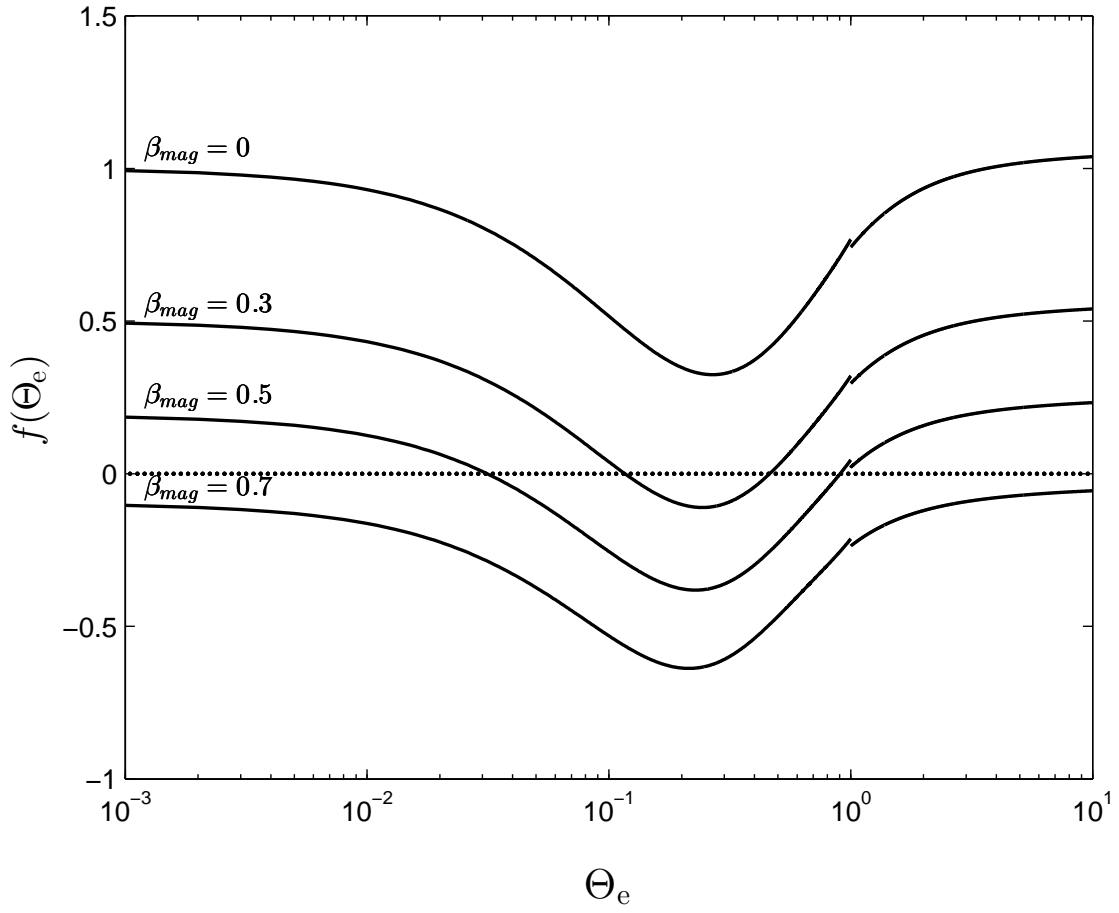


Fig. 1.— Variation of the function $f(\Theta_e)$ for $\beta_{mag} = 0, 0.3, 0.5$, and 0.7 .

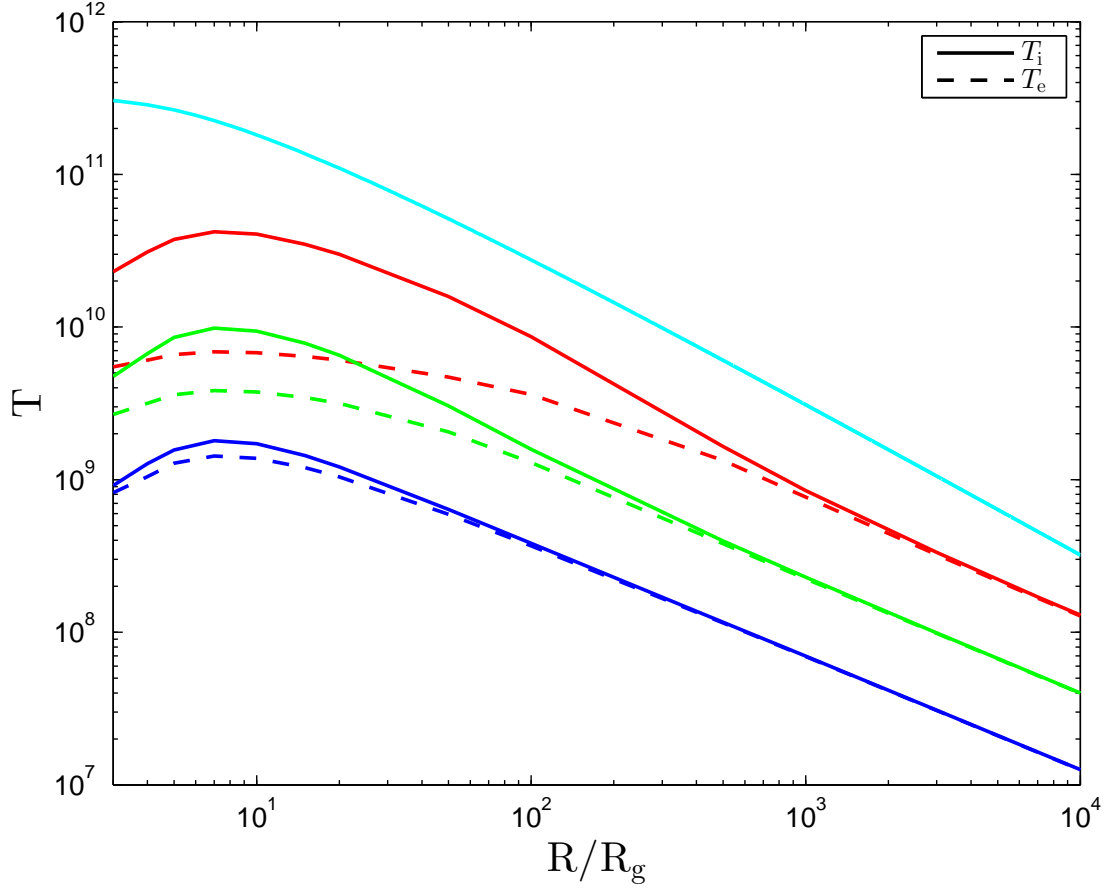


Fig. 2.— Radial variations of the ion temperature T_i (solid) and the electron temperature T_e (dashed) for $m = 0.001$ (blue), 0.01 (green), and 0.1 (red), where $\beta_{\text{mag}} = 0.5$. The navy blue solid line represents the theoretical ion temperature of ADAF (Equation 24).

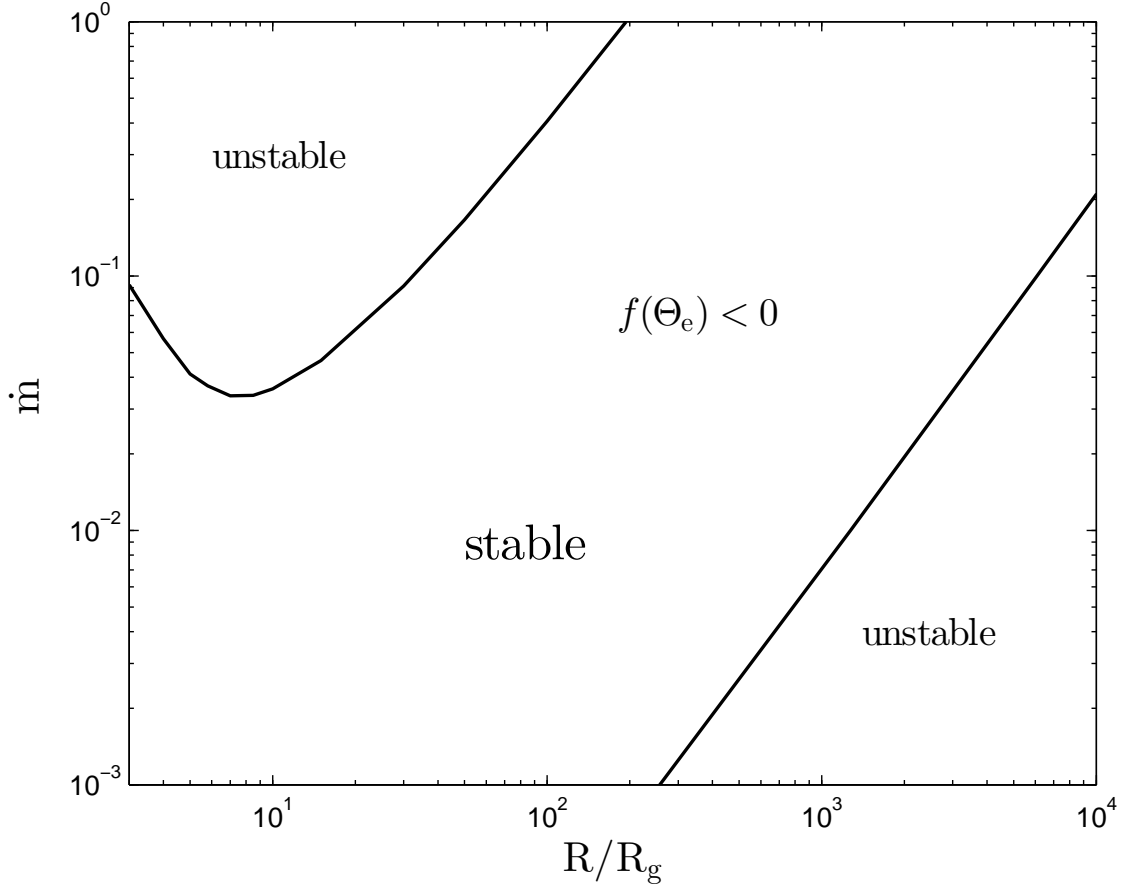


Fig. 3.— The $\dot{m} - R$ diagram for the thermal stability, where $\beta_{\text{mag}} = 0.5$.